

¹³C Line Narrowing by ²H Decoupling in ²H/¹³C/¹⁵N-Enriched Proteins. Application to Triple Resonance 4D J Connectivity of Sequential Amides

Stephan Grzesiek,[†] Jacob Anglister,^{†,‡} Hao Ren,[§] and Ad Bax^{*,†}

Laboratory of Chemical Physics, National Institute of Diabetes and Digestive and Kidney Diseases, and Laboratory of Biochemistry, National Cancer Institute
National Institutes of Health, Bethesda, Maryland 20892

Received February 3, 1993

Short transverse ¹³C relaxation times, T_2 , constitute the principal barrier for the application of heteronuclear J correlation NMR techniques to larger proteins uniformly enriched with ¹³C and ¹⁵N.^{1–6} The ¹³C T_2 is dominated by the strong dipolar interaction with its attached protons.⁷ As the magnetogyric ratio of ²H is ~6.5 times lower than that of ¹H, the heteronuclear dipolar interaction is greatly reduced by deuteration. Because of the large ²H quadrupolar interaction (~170 kHz), the ²H spin lattice relaxation time, T_1 , in proteins is in the millisecond range at a magnetic field strength of 14 T. Therefore, the ²H–¹³C J coupling (~22 Hz) does not result in the triplet shape, expected for a ¹³C nucleus coupled to a spin-1 nucleus, but gives rise to a collapsed singlet resonance that is broadened by scalar relaxation of the second kind.^{8,9} High-power (~2.5 W) ²H decoupling with an RF field strength much stronger than the inverse ²H T_1 effectively removes this broadening and results in a ¹³C line width that is much narrower than for the protonated ¹³C.

One of the triple resonance J correlation experiments affected most by the ¹³C line width is the H(CA)NH experiment^{10,11} which relies on magnetization transfer from C $^\alpha$ to the backbone ¹⁵N nucleus via the relatively small $J_{\text{NC}\alpha}$ (~11 Hz) and $J_{\text{NC}\beta}$ (~5–8 Hz)¹² couplings. Although experiments have been proposed to alleviate this difficult J correlation step,^{13,14} the sequential assignment procedure which is based on J correlation between the intrasidue ¹H/¹⁵N and ¹H/¹³C $^\alpha$ resonances and between the ¹H/¹³C $^\alpha$ of residue i and ¹H/¹⁵N of residue $i + 1$ is complicated by the high degree of overlap among ¹H/¹³C $^\alpha$ correlations. Here we describe a procedure which allows J correlation between the much better resolved ¹H/¹⁵N resonances of sequential residues, thereby bypassing the overlapping ¹H/¹³C $^\alpha$ pairs. Efficient transfer of magnetization from ¹³C $^\alpha$ to ¹⁵N is possible in the present case because of the ¹³C $^\alpha$ line narrowing afforded by deuteration and ²H decoupling.

Briefly the scheme of Figure 1 functions as follows. After HN_{i+1} evolution during t_1 , magnetization is transferred to its attached nucleus N_{i+1} (time a). Following a constant time evolution period, t_2 , during which ¹³C $^\alpha$ is decoupled from ¹⁵N, the ¹⁵N $_{i+1}$ magnetization is relayed via ¹³CO $_i$ (time b) and ¹³C $^\alpha_i$ magnetization (time c) to the ¹⁵N $_i$ of residue i (time d). The effect of dephasing caused by the homonuclear ¹³C $^\alpha$ –¹³C $^\beta$ J coupling during the period where C $^\alpha$ magnetization is transverse ($\eta = \eta_1 + \eta_2 + \eta_3$) is effectively eliminated by setting η to $\sim 1/J_{\text{CC}}$ (27.6 ms). At time d , a fraction $\sin[\pi\eta(^1J_{\text{NC}\alpha})] \cos[\pi\eta(^2J_{\text{NC}\alpha})]$ of the C $^\alpha$ magnetization is transferred to the intrasidue ¹⁵N, and a smaller fraction, $\sin[\pi\eta(^2J_{\text{NC}\alpha})] \cos[\pi\eta(^1J_{\text{NC}\alpha})]$, is transferred back to the amide from which magnetization originated. After the second ¹⁵N constant time evolution period, t_3 , (time e), magnetization is transferred by means of a reverse INEPT sequence to HN for observation. In the 4D spectrum, the frequency coordinates of J correlations in the F_1 , F_2 , F_3 , and F_4 dimensions then correspond to the chemical shifts of HN_{i+1} , N_{i+1} , N_i , and HN_i , respectively. The “diagonal peaks” at HN_{i+1} , N_{i+1} , HN_{i+1} , and N_{i+1} , due to the above mentioned two-bond $J_{\text{NC}\alpha}$ transfer process, are 2–4 times weaker.

Experiments are conducted on a Bruker AMX-600 spectrometer, modified such that the ²H lock receiver is disabled during ²H decoupling. Details regarding this hardware modification will be published elsewhere. The method is demonstrated for a sample containing ~1.4 mM of the protein calcineurin B (19.7 kD), uniformly enriched with ²H, ¹⁵N, and ¹³C to levels of 50%, 98%, and 88%, respectively. A second sample, with higher deuteration (~85%), was also prepared to illustrate directly the ¹³C line narrowing obtainable. The fact that the deuteration level of the sample used for the 4D experiment is only 50% lowers the sensitivity of this particular experiment, but it permits this sample to be used also for a large range of other experiments that require partial side-chain protonation. Both samples also contain 20 mM CaCl₂ and 20 mM CHAPS, a zwitterionic detergent which was shown not to significantly affect the structure or binding affinity of calcineurin B.¹⁵ Experiments were conducted at 37 °C, pH 5.6.

Figure 2 illustrates the ¹³C resolution enhancement obtained by deuteration and ²H decoupling for a small region of the 2D H(N)CA correlation spectrum,¹⁶ displaying connectivities between amide protons and their intrasidue C $^\alpha$. In the absence of deuteration and ²H decoupling, the ¹³C $^\alpha$ resonance is a poorly resolved doublet, split by J_{CC} coupling with ¹³C $^\beta$, with a line width for the doublet components of ca. 25 Hz (Figure 2A). In the case of deuteration and ²H decoupling, the C $^\alpha$ doublet is well-resolved with line widths of ~10 Hz (Figure 2B). The ¹³C $^\alpha$ resonances in the deuterated protein are shifted upfield by ~0.35 ppm, caused primarily by the one-bond ²H isotope effect. The 10-Hz ¹³C $^\alpha$ line width is determined primarily by the limited acquisition time in the t_1 dimension of the 2D H(N)CA experiment, and by incomplete deuteration of the amino acid side chains which results in a distribution of two- and three-bond isotope effects.

Figure 3 shows four cross sections through the 4D HN(COCA)-NH spectrum, illustrating J connectivities between the amides of residues F72–F75. Of all the sequential J connectivities expected on the basis of the backbone assignments,¹⁷ 98% were observed, except for a stretch of residues close to the C154K mutation, which causes line broadening of the resonances.¹⁷

Previous attempts to demonstrate the ¹³C line narrowing

- [†] National Institute of Diabetes and Digestive and Kidney Diseases.
[‡] On leave from The Weizmann Institute, Rehovot, Israel.
[§] National Cancer Institute.
(1) Oh, B. H.; Westler, W. M.; Derba, P.; Markley, J. L. *Science* **1988**, *240*, 908–911.
(2) Ikura, M.; Kay, L. E.; Bax, A. *Biochemistry* **1990**, *29*, 4659–4667.
(3) Boucher, W.; Laue, E. D.; Campbell-Burk, S.; Domaile, P. J. *J. Am. Chem. Soc.* **1992**, *114*, 2262–2264.
(4) Olejniczak, E. T.; Xu, R. X.; Fesik, S. W. *J. Biomol. NMR* **1992**, *2*, 655–659.
(5) Palmer, A. G., III; Fairbrother, W. J.; Cavanagh, J.; Wright, P. E.; Rance, M. *J. Biomol. NMR* **1992**, *2*, 103–108.
(6) Grzesiek, S.; Döbeli, H.; Gentz, R.; Garotta, G.; Labhardt, A. M.; Bax, A. *Biochemistry* **1992**, *31*, 8180–8190.
(7) Browne, D. T.; Kenyon, G. L.; Packer, E. L.; Sternlicht, H.; Wilson, D. M. *J. Am. Chem. Soc.* **1973**, *95*, 1316–1323.
(8) Abragam, A. *The Principles of Nuclear Magnetism*; Clarendon Press: Oxford, 1961; p 309.
(9) London, R. E. *J. Magn. Reson.* **1990**, *86*, 410–415.
(10) Montelione, G. T.; Wagner, G. *J. Magn. Reson.* **1990**, *87*, 183–188.
(11) Kay, L. E.; Ikura, M.; Bax, A. *J. Magn. Reson.* **1991**, *91*, 84–92.
(12) Delaglio, F.; Torchia, D. A.; Bax, A. *J. Biomol. NMR* **1991**, *1*, 439–446.
(13) Clubb, R. T.; Thanabal, V.; Wagner, G. *J. Biomol. NMR* **1992**, *2*, 203–210.
(14) Clubb, R. T.; Thanabal, V.; Wagner, G. *J. Magn. Reson.* **1992**, *97*, 213–217.

- (15) Anglister, J.; Grzesiek, S.; Ren, H.; Klee, C. B.; Bax, A. *J. Biomol. NMR* **1993**, *3*, 121–126.
(16) Grzesiek, S.; Bax, A. *J. Magn. Reson.* **1992**, *96*, 432–440.
(17) Anglister, J.; Grzesiek, S.; Ren, H.; Klee, C. B.; Bax, A. Unpublished results.
(18) LeMaster, D. M.; Richards, F. M. *Biochemistry* **1988**, *27*, 142–150.
(19) Shaka, A. J.; Lee, C. J.; Pines, A. *J. Magn. Reson.* **1988**, *77*, 274–293.
(20) Bax, A.; Pochapsky, S. S. *J. Magn. Reson.* **1992**, *99*, 638–643.

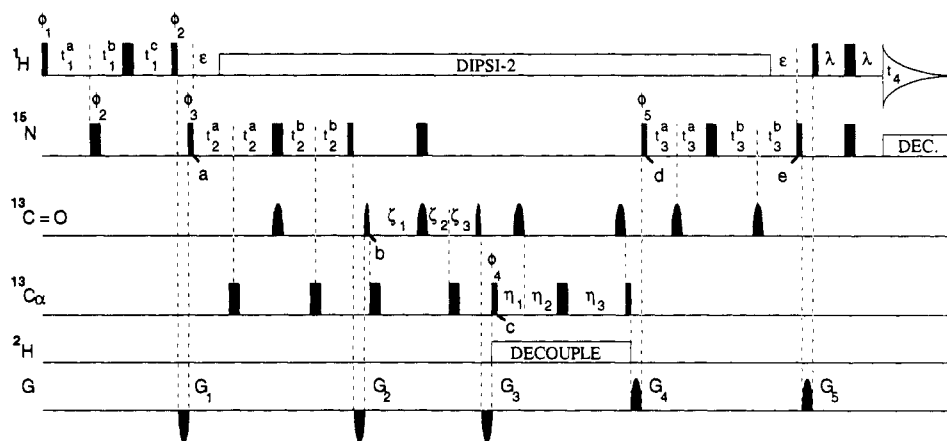


Figure 1. Pulse scheme of the HN(COCA)NH experiment. Narrow pulses correspond to a flip angle of 90° , wide pulses to 180° . Pulses for which the RF phase is not marked are applied along the x axis. Carbonyl pulses have a $\sin x/x$ -center-lobe amplitude profile. Carrier frequencies are set to 4.66, 116.5, 177, 56, and 4 ppm for the ^1H , ^{15}N , $^{13}\text{C}=\text{O}$, $^{13}\text{C}\alpha$, and ^2H nuclei, respectively. ^1H and ^{15}N pulses are applied at 25 and 6 kHz, whereas the $^{13}\text{C}\alpha$ ($^{13}\text{C}=\text{O}$) 90° and 180° pulses have durations of 53 and 47.4 μs (219 and 300 μs), respectively. The ^1H decoupling (DIPSI-2)¹⁹, ^{15}N (WALTZ-16), and ^2H (cw) decoupling are applied at field strengths of 5, 1.5, and 1.6 kHz, respectively. Phase cycling is as follows: $\phi_1 = x$; $\phi_2 = y, -y$; $\phi_3 = x$; $\phi_4 = 2(x), 2(-x)$; $\phi_5 = x$; $\text{acq} = x, 2(-x), x$. Pulsed field gradients are used to suppress artifacts, not to select a coherence transfer pathway.²⁰ Gradients have a sine bell amplitude profile with a strength of 10 G/cm at their center. Durations are $G_{1,2,3,4,5} = 0.85, 0.25, 0.35, 1.50, 4.00$ ms. Quadrature in the t_1, t_2 , and t_3 domains is obtained by changing the phases ϕ_1, ϕ_3 , and ϕ_5 , respectively, in the usual states-TPP1 manner.²¹ Delay durations are as follows: $\epsilon = 5.4$ ms; $\lambda = 2.25$ ms; $\zeta_{1,2,3} = 11.1, 6.5, 4.6$ ms; $\eta_{1,2,3} = 4.8, 9.0, 13.8$ ms. The initial delays for the semi-constant-time²² evolution period (t_1) and constant time evolution periods (t_2 and t_3) are set to $t_{1^{a,b,c}} = 2.25, 0, 2.25$ ms; $t_{2^{a,b}} = 5.6$ ms; $t_{3^{a,b}} = 6.8$ ms. Increments for those delays are set to $\Delta t_{1^{a,b,c}} = 354, 204, -102$ μs ; $\Delta t_{2^{a,b}} = 275, -275$ μs ; $\Delta t_{3^{a,b}} = 275, -275$ μs .

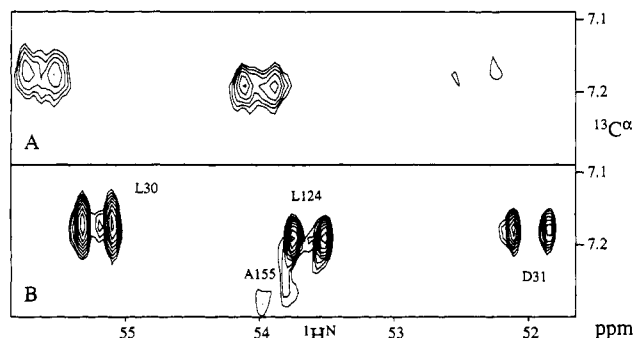


Figure 2. Small regions of the 2D H(N)CA spectrum of (A) fully protonated calcineurin B and (B) randomly 85%-deuterated calcineurin B, with ^2H decoupling. Both spectra were recorded and processed identically. The t_1 and t_2 acquisition times used are 73 and 55 ms, respectively, and data are zero filled to yield a digital resolution of 5 Hz (F_1) and 9 Hz (F_2), with no digital filtering in the t_1 dimension.

obtained by deuteration and ^2H decoupling were only partially successful because the rapid ^2H spin lattice relaxation at the low magnetic field strength used (1.4 T) required a stronger ^2H decoupling field than could be generated experimentally.⁷ At the high magnetic field strength used in our present work (14 T), ^2H T_1 relaxation is much longer, and in addition, the ^2H decoupling field used in our study is nearly 7 times stronger.

Random fractional deuteration, previously explored in homonuclear ^1H NMR,¹⁸ presents a powerful approach for overcoming the natural line width problem in heteronuclear NMR studies of larger $^{13}\text{C}/^{15}\text{N}$ -enriched proteins. The present experiment is only a single example of the utility of this approach, but a large range of experiments that can benefit from deuteration is presently under investigation.

Acknowledgment. We thank Claude Klee for enthusiastic support of the calcineurin B NMR study, Geerten Vuister and

(21) Marion, D.; Ikura, M.; Tschudin, R.; Bax, A. *J. Magn. Reson.* **1989**, *85*, 393-399.

(22) Grzesiek, S.; Bax, A. *J. Biomol. NMR* **1993**, *3*, 185-204.

(23) Zhu, G.; Bax, A. *J. Magn. Reson.* **1990**, *90*, 405-410.

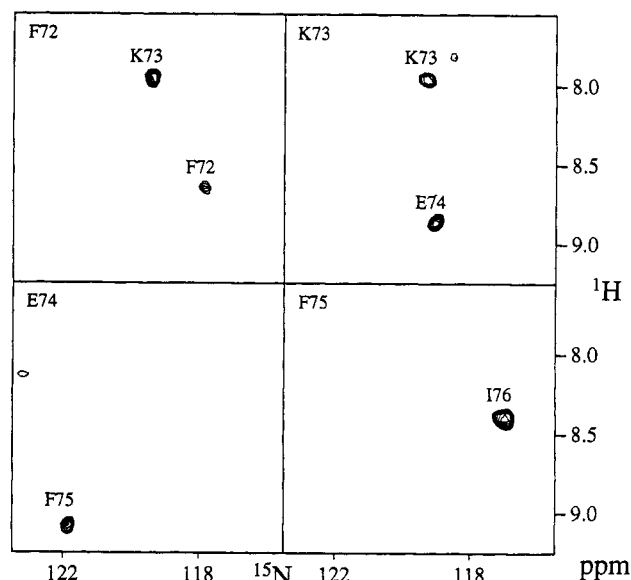


Figure 3. Four (F_1, F_2) cross sections through the 4D HN(COCA)NH spectrum of calcineurin B (50% ^2H), taken at the (F_3, F_4) frequencies of the amides of residues F72-F75. Each cross section shows the connection to amide ^{15}N and ^1H frequencies of the next residue; panels for F72 and K73 also show the weaker (4D) diagonal peaks to the same residue. The 4D spectrum results from a $22^* \times 20^* \times 24^* \times 512^*$ data matrix, where n^* refers to n complex data points. Total accumulation time was 6 days with 32 scans per hypercomplex t_1, t_2, t_3 -increment. Acquisition times were 14.5 ms (t_1), 22.0 ms (t_2), 26.4 ms (t_3), and 55.3 ms (t_4). The t_2 and t_3 time domains were extended by means of mirror image linear prediction²³ prior to zero filling and Fourier transformation. The size of the absorptive part of the final 4D spectrum was $64 \times 128 \times 128 \times 1024$.

Andy Wang for useful comments, and Rolf Tschudin for spectrometer hardware modification. This work was supported by the Intramural AIDS Targeted Anti-Viral Program of the Office of the Director of the National Institutes of Health.